Supplementary Information

Application of mitochondrially targeted nanoconstructs to neo-adjuvant X-ray-induced photodynamic therapy for rectal cancer

Wei Deng *[1], Kelly J McKelvey[2#], Anna Guller[1,3#], Alexey Fayzullin[1,3], Jared M Campbell[1], Sandhya Clement[1], Abbas Habibalahi[1], Zofia Wargocka[1], Liuen Liang[4], Chao Shen[5], Viive Maarika Howell[2], Alexander Frank Engel [6,7] and Ewa M Goldys *[1]

[1]ARC Centre of Excellence for Nanoscale Biophotonics, Graduate School of Biomedical Engineering, University of New South Wales, Kensington, New South Wales 2052, Australia

[2]Bill Walsh Translational Cancer Research Laboratory, The Northern Clinical School, Faculty of Medicine and Health, The University of Sydney and Northern Sydney Local Health District Research (Kolling Institute), St Leonards, New South Wales, 2065, Australia.

[3]Institute for Regenerative Medicine, Sechenov First Moscow State Medical University (Sechenov University), Moscow,119991, Russia

[4]Department of Physics and Astronomy, Faculty of Science and Engineering, Macquarie University, North Ryde, New South Wales 2109, Australia

[5]Faculty of Science and Engineering, Macquarie University, North Ryde, New South Wales 2109, Australia.

[6]Sydney Medical School, University of Sydney, Sydney, New South Wales 2006, Australia.

[7]Department of Colorectal Surgery, Royal North Shore Hospital, St Leonards, New South Wales 2065, Australia.

[#] These authors contributed equally to this work

E-mail: wei.deng@unsw.edu.au; E-mail: e.goldys@unsw.edu.au

Quantification of singlet oxygen generation from PLGA nanocarriers loaded with gold and verteporfin (PLGA-VP-Au) with X-ray excitation:

The singlet oxygen generation in this work is monitored using a fluorescent probe called Singlet oxygen sensor green (SOSG). In order to calculate the number of singlet oxygen generated, we need to establish a relation between the SOSG intensity, and the number of singlet oxygen generated. We already established a method and implemented the same in our previous works [1-4].

In order to calculate the number of singlet oxygen generated from the SOSG intensity, a known singlet oxygen quantum yield (SOQY) value of verteporfin (VP) and corresponding singlet oxygen generation values are required. We already calculated the SOQY of VP at 365 nm wavelength and was 0.53 ± 0.06 [2]. Herein, we tried to find out the SOQY enhancement in the case of PLGA-VP-Au compared to PLGA-VP at this wavelength (365 nm) to know the enhancement contribution of Au to PLGA-VP. Also, we are assuming that SOQY of PLGA-VP is the same as that of VP at this wavelength as PLGA does not have any role in singlet oxygen generation. The SOQY of PLGA-VP-Au was calculated using the equation

$$\phi_{PLGA-VP-Au} = \phi_{PLGA-VP}^{\frac{r_{PLGA-VP-Au}}{(1-T_{PLGA-VP-Au})}} \Big/ \frac{r_{PLGA-VP}}{(1-T_{PLGA-VP})} \quad (1)$$

Where ϕ denotes the SOQY, r denotes the reaction rate of the SOSG probe with singlet oxygen generation and T is the transmittance value at 365 nm. Figure S1 (a) shows the absorption spectra corresponding to both PLGA and PLGA-VP. The T of both the samples can be calculated from the absorbance (A) values using the equation

$$T = 10^{-A} \quad (2)$$

and the r values can be obtained from Figure S1 (b). So, the SOQY of PLGA-VP-Au calculated using the above equations and is estimated as 1.2289±0.02. In this case the enhancement factor was around 2.3 and is comparable with the previous literature values [2]. So, this enhancement factor gives a foundation for using Au in conjugation with PLGA-VP for our X-ray studies.

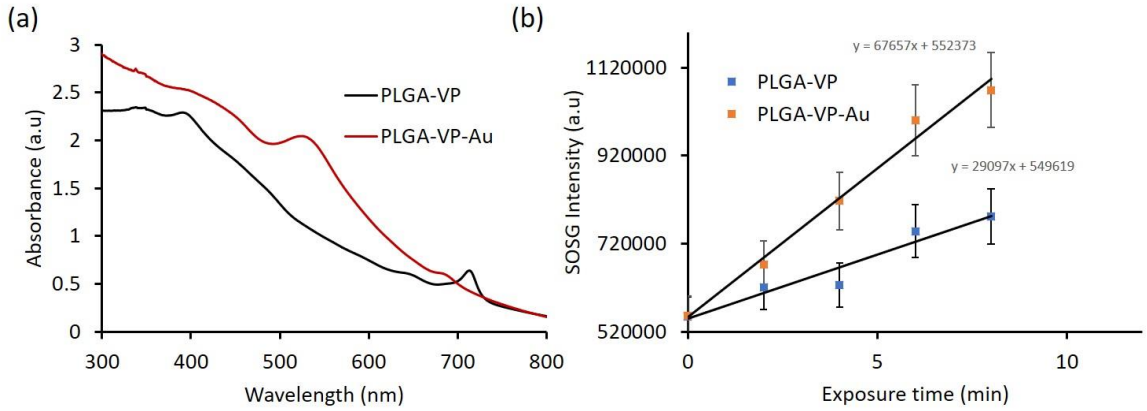

Figure S1. (a) absorption spectra of PLGA-VP and PLGA-VP-Au; (b) Singlet oxygen generation from PLGA-VP and PLGA-VP-Au with 365 nm LED for different time points. Values represent the means ± standard deviation of three experiments.

The number of singlet oxygen generation from PLGA-VP and PLGA-VP-Au are calculated based on combining the singlet oxygen generation data from both 365 nm and X-ray radiation. Firstly, the number of UV photons absorbed ($N_{uv}(t)$) from 365 nm by PLGA-VP can be calculated using the equation

$$N_{uv}(t) = ({}^{P}/_{E}) \times F \times t \qquad (3)$$

Where P is the power of the UV lamp at 365 nm (61 mW), E is the energy of the UV photon, F is the absorption factor of PLGA-VP at 365 nm (1.9802) and t is the UV exposure time in seconds. This $N_{uv}(t)$ is calculated and plotted as a function n of t as shown in Figure S2 (b). From this data, it is possible for us to calculate the No. of singlet oxygen generated (N_{so}) using the equation

$$\phi = {}^{N_{so}}/_{N_{uv}} \qquad (4)$$

This N_{so} calculated can be compared with SOSG intensity in figure 1(b) and can be redrawn as shown in figure 2 (b). So, from this figure 2(b), We are getting a conversion factor of 3×10^{14} to convert the SOSG intensity to number of singlet oxygen generated.

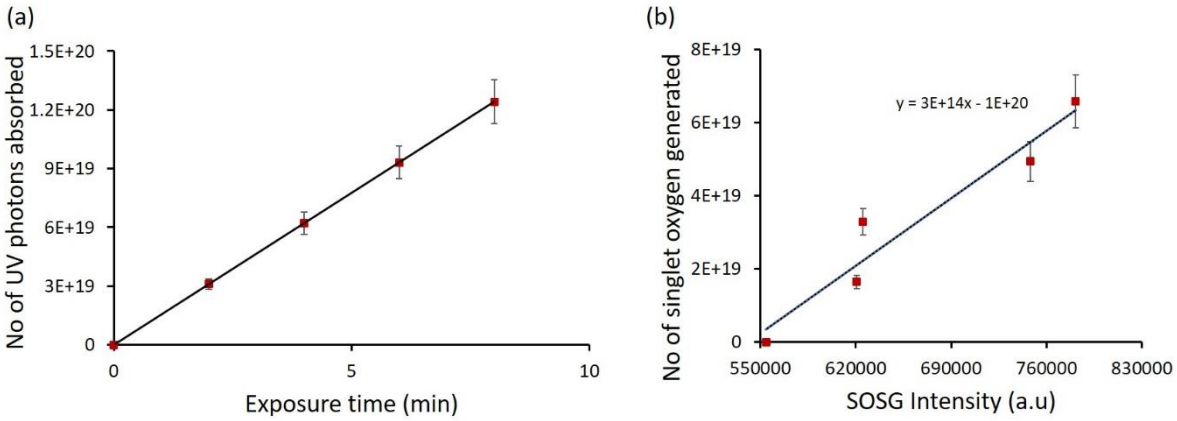

Figure S2. (a) Calculated number of UV photons absorbed as a function of exposure time; (b) Number of singlet oxygen generated corresponding to the SOSG intensity under UV excitation. Values represent the means ± standard deviation of three experiments.

Applying this conversion factor to the SOSG intensity obtained for X-ray radiation, we are able to calculate the number of singlet oxygen generated from both PLGA-VP and PLGA-VP-Au at different radiation dose (Figure S3). For example, the singlet oxygen generated from PLGA-VP at 4 Gy is around 1.58×10^{20} whereas PLGA-VP-Au generate 2.10×10^{20}. Here, the singlet oxygen generation has an enhancement factor of 1.3 in the presence of gold with 4 Gy X-ray dose. These total number of singlet oxygen generated is on a 3 ml solution of PLGA-VP/PLGA-VP-Au with a concentration of VP as 0.011 mg/ml.

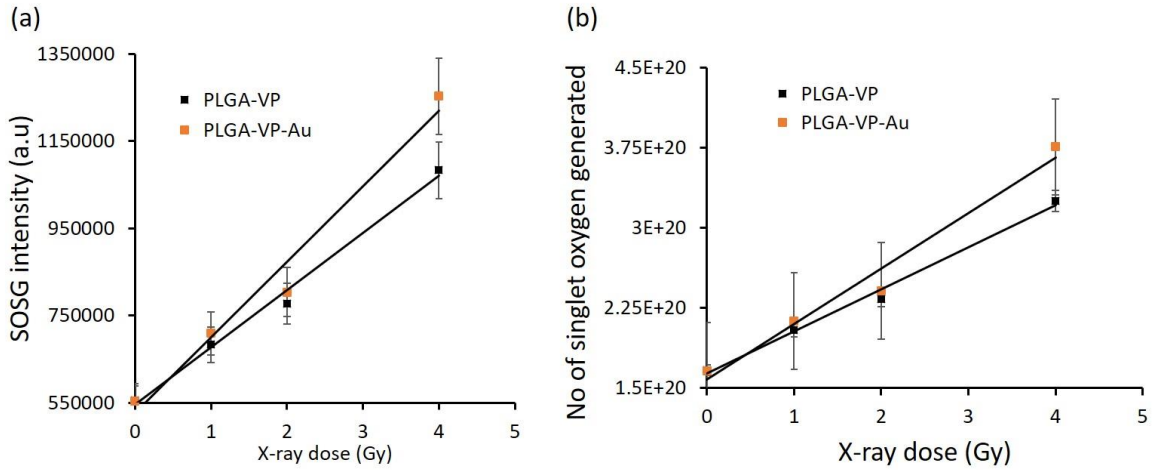

Figure S3. (a) SOSG fluorescence intensity variation as a function radiation dose for PLGA-VP and PLGA-VP-Au; (b) Calculated number of singlet oxygen generated as a function of radiation dose for PLGA-VP and PLGA-VP-Au. Values represent the means ± standard deviation of three experiments.

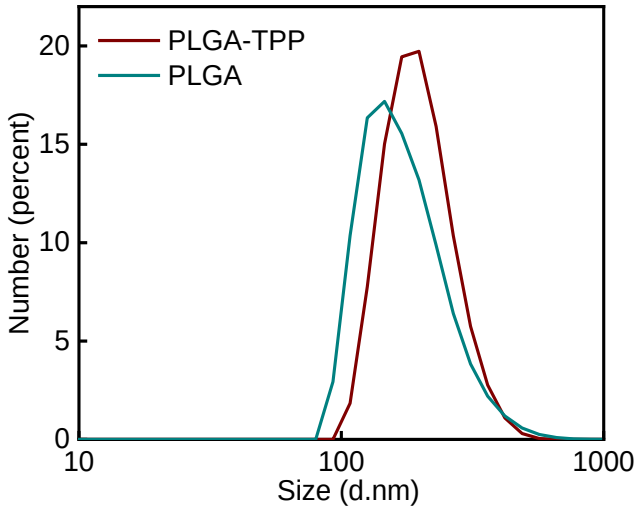

Figure S4 The size distribution of PLGA with and without TPP modification

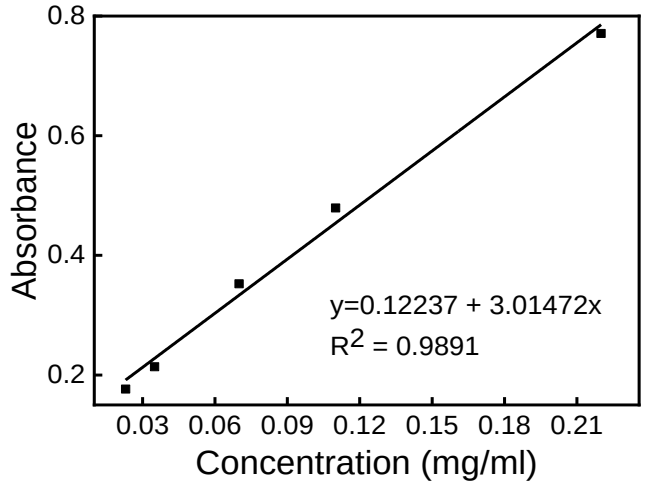

Figure S5 Standard curve of absorbance versus concentration of carboxyl-terminated TPP solution.

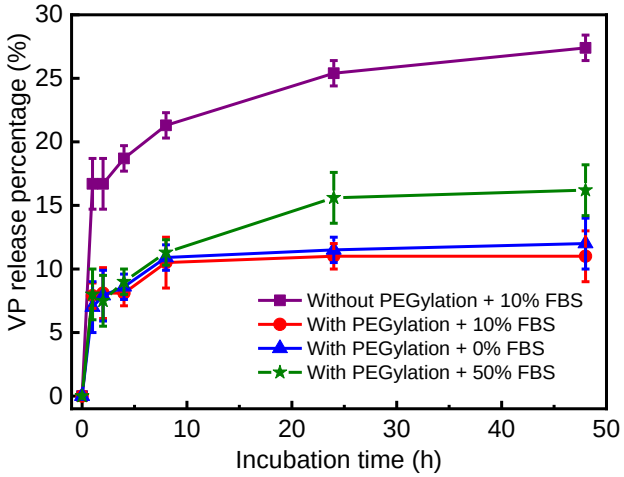

Figure S6 The percentage of released VP from PLGA samples incubated in PBS (pH 7.4) with 0%, 10% and 50% FBS.

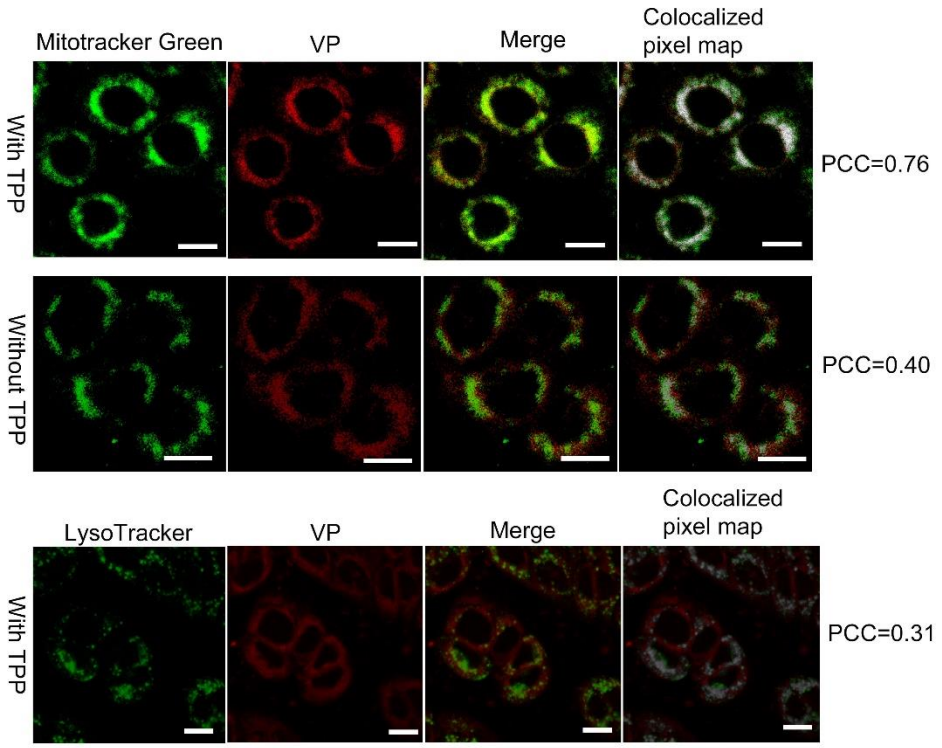

Figure S7. Confocal micrographs of HCT116 cells after 4 hr incubation with PLGA-TPP and PLGA nanocarriers. Mitochondria were stained by 200 nM MitoTracker Green for 20 min. Lysosomes were stained with 200 nM LysoTracker Red (green pseudocolor). Scale bar is 20 microM. Quantitative analysis was conducted using the ImageJ/Fiji "colocalization analysis" function.

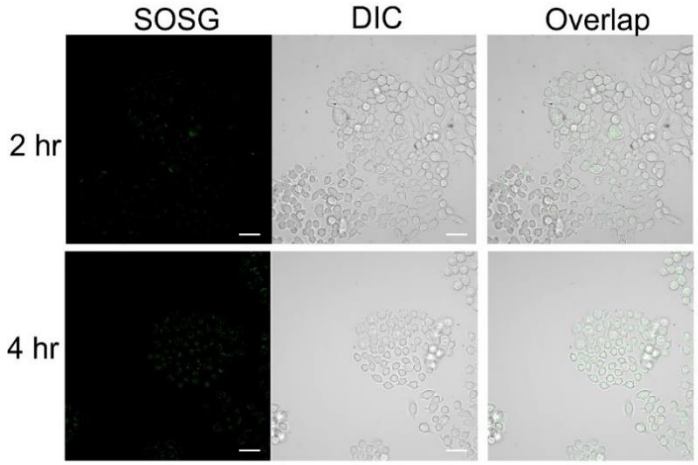

Figure S8 The confocal laser scanning microscopy images of SOSG in HCT116 cells obtained at 2 hr and 4 hr after the treatment with X-ray triggered PLGA-TPP. Scale bar is 50μm.

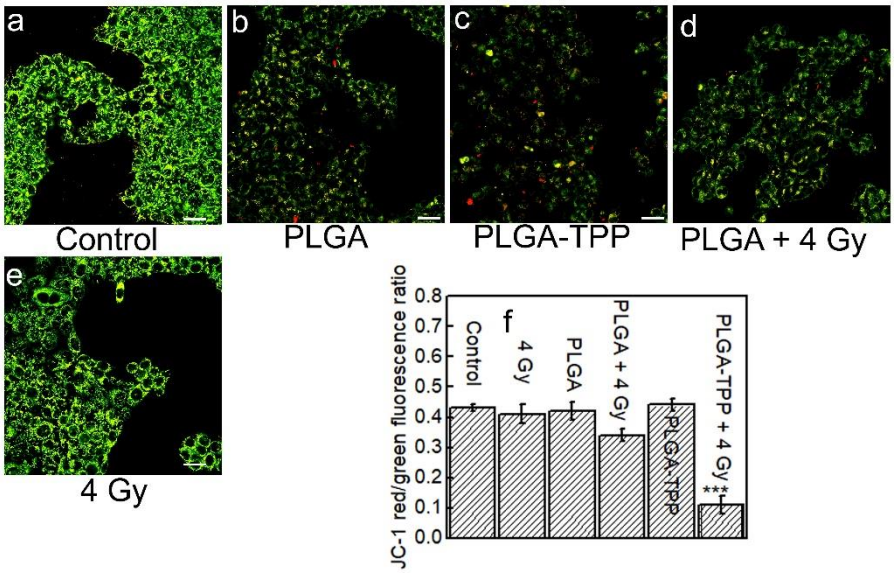

Figure S9 Representative confocal images detection of $\Delta\psi_m$ in HCT116 cells at 24 hr (a) without treatment, after the treatment with (b) PLGA nanocarriers, (c) PLGA-TPP nanocarriers, (d) PLGA nanocarriers in combination with 4 Gy radiation and (e) 4 Gy radiation alone. (f) The levels of membrane potential are indicated by red fluorescence intensity versus green fluorescence intensity in the cells. Scale bar is 50 μm. *** $p<0.001$, compared with other treatment groups (n=4).

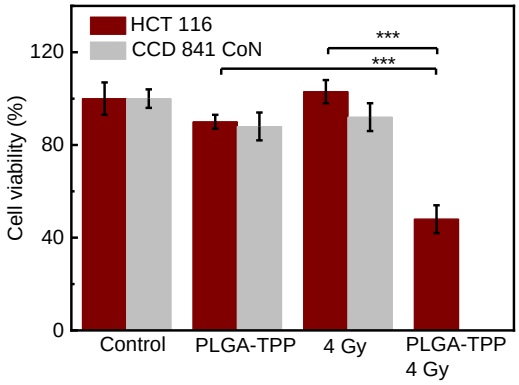

Figure S10 Cell-killing effect of PLGA-TPP nanocarriers on HCT116 and CCD 841 CoN cells without and with X-ray radiation at 24 hr. The concentration of PLGA-TPP was 50 μg/mL. The viabilities are expressed as mean percentages and standard deviation (n=4) relative to control cells. *** $p<0.001$.

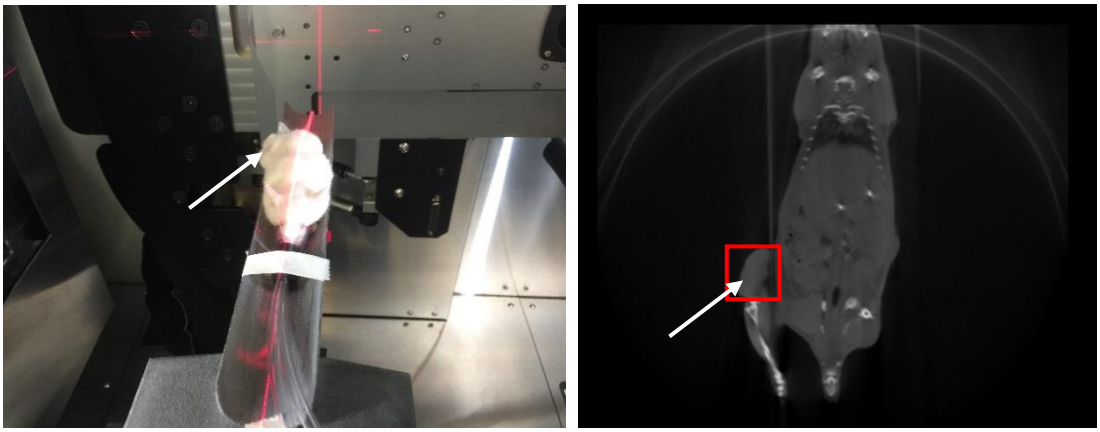

Figure.S11 (a) *In vivo* X-ray radiation setup prior to dose delivery to the mouse. (b) CT image of the same mouse. White arrows denote the location of the subcutaneous tumour. Red box denotes the positioning of the 10 × 10 mm radiation field.

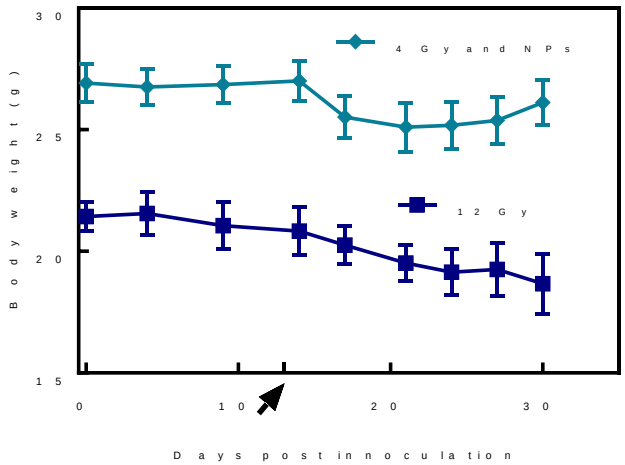

Figure S12 Changes of mouse body weight after a single 12 Gy radiation and X-ray triggered PDT as indicated. A black arrow indicates the time of treatment administration. Error bars show standard deviation from four (n=4 for the 12 Gy treatment) or five (n=5 for X-ray triggered PDT) experiments.

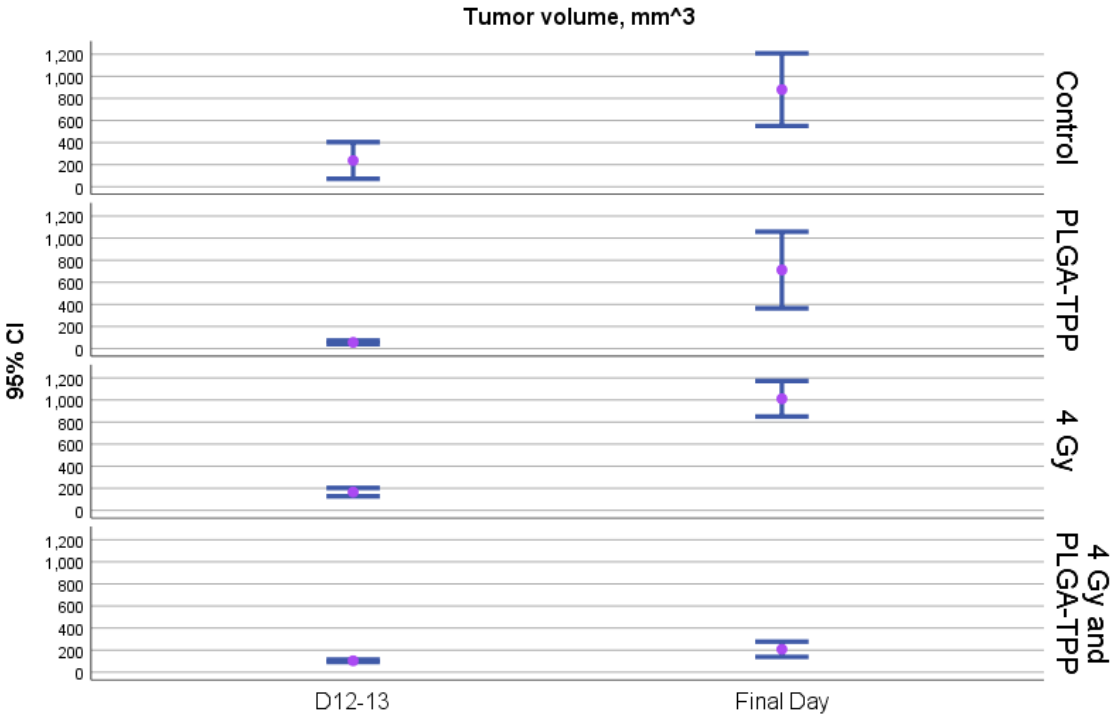

Figure S13 Tumour volume on Day 12-13 and the day of the animals' death/ end day of the experiment.

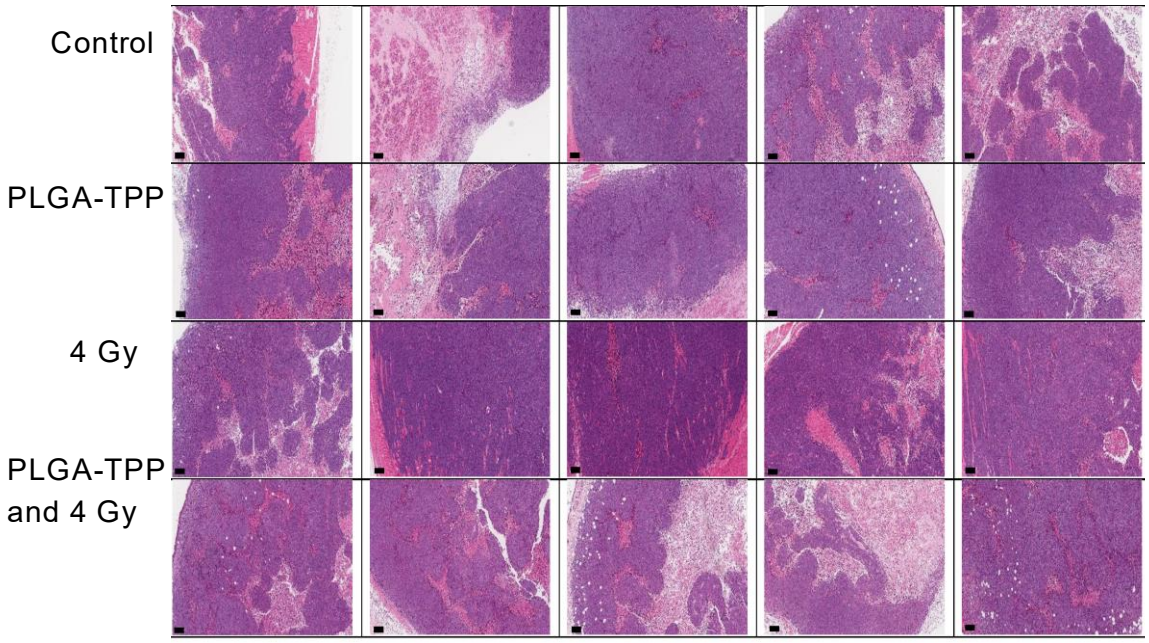

Figure S14 Histological structure of the tumours in the studied groups. H&E staining, magnification ×400, scale bar 50 μm.

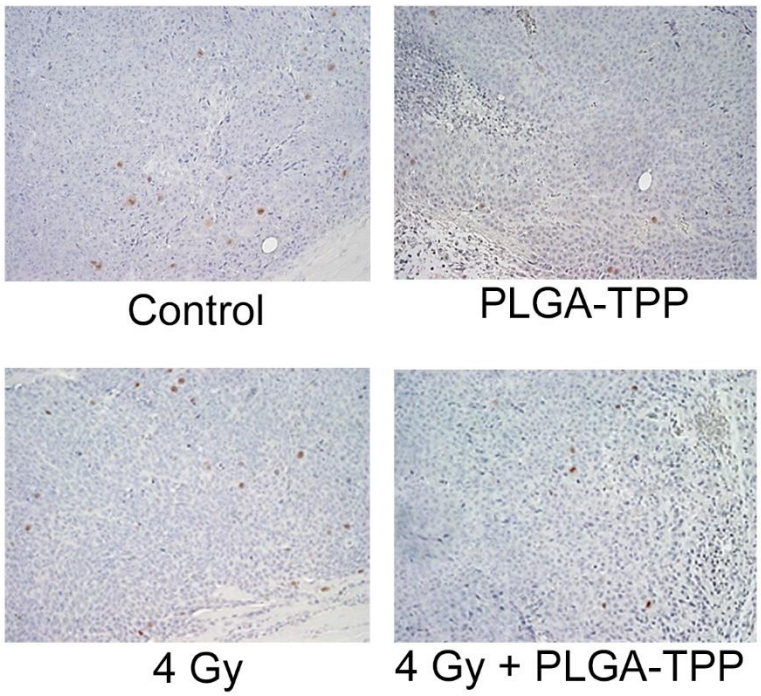

Figure S15 The representative stained sections of control and treated tumours for Ki-67

Table S1a. Kruskall-Wallis test of the fibrotic signs in the tumours. Ranks.

	Group	N	Mean Rank
Fibrotic capsule volume, scores	Control	10	13.30
	PLGA-TPP	10	23.90
	4 Gy	10	10.70
	4 Gy and PLGA-TPP	10	34.10
	Total	40	
Fibrotic capsule collagen staining intensity, scores	Control	10	16.50
	PLGA-TPP	10	22.95
	4 Gy	10	10.10
	4 Gy and PLGA-TPP	10	32.45
	Total	40	
Collagen staining intensity in the central necrotic area, scores	Control	10	14.60
	PLGA-TPP	10	24.60
	4 Gy	10	10.45
	4 Gy and PLGA-TPP	10	32.35
	Total	40	

Table S1b. Kruskall-Wallis test of the fibrotic signs in the tumours. Test Statistics [a,b]

	Fibrotic capsule volume, scores	Fibrotic capsule collagen staining intensity, scores	Collagen staining intensity in the central necrotic area, scores
Kruskal-Wallis H	27.866	21.585	23.253
df	3	3	3
Asymp. Sig.	.000	.000	.000

a. Kruskal Wallis Test

b. Grouping Variable: Group

Reference:

1. Clement, S., et al., *X-ray induced singlet oxygen generation by nanoparticle-photosensitizer conjugates for photodynamic therapy: determination of singlet oxygen quantum yield.* Scientific reports, 2016. **6**: p. 19954.
2. Clement, S., et al., *Nanoparticle-mediated singlet oxygen generation from photosensitizers.* Journal of Photochemistry and Photobiology A: Chemistry, 2017. **332**: p. 66-71.
3. Kautzka, Z., et al., *Light-triggered liposomal cargo delivery platform incorporating photosensitizers and gold nanoparticles for enhanced singlet oxygen generation and increased cytotoxicity.* International journal of nanomedicine, 2017. **12**: p. 969.
4. Deng, W., et al., *Controlled gene and drug release from a liposomal delivery platform triggered by X-ray radiation.* Nature communications, 2018. **9**(1): p. 2713.